Effect of Monomer Concentration on Propene Polymerization with the *rac*-[Ethylenebis(1-indenyl)]zirconium Dichloride/Methylaluminoxane Catalyst[1]

Luigi Resconi,* Anna Fait, Fabrizio Piemontesi, and Marcello Colonnesi

Montell Polyolefins, G. Natta Research Center, P. le G. Donegani 12, 44100 Ferrara, Italy

Helena Rychlicki and Robert Zeigler

Montell Polyolefins, Research & Development Center, 912 Appleton Road, Elkton, Maryland 21921

Received June 2, 1995[⊗]

ABSTRACT: The structural details of isotactic polypropene (iPP) produced with the moderately isospecific *racemic*-ethylenebis(1-indenyl)zirconium dichloride/methylaluminoxane (*rac*-(EBI)$ZrCl_2$/MAO) catalyst are strongly dependent on monomer concentration. Polymerizing propene at 50 °C in toluene, at propene concentrations in the experimentally measurable range 0.4–11 mol/L, *rac*-(EBI)$ZrCl_2$/MAO shows activities in the range 2–350 $kg_{PP}/(mmol_{Zr} \cdot h)$ and yields polypropenes with $\bar{M}_v$'s from 8800 to 36 600, percent mmmm pentads ranging from 54 to 86%, and corresponding melting temperatures from 86 to 136 °C. Two types of regioirregular (secondary) placements in an isotactic sequence of primary propene insertions are observed in iPP synthesized in liquid monomer, erythro (E, ca. 0.4%) and threo (T, ca. 0.2%). These secondary units are gradually converted into 1,3 propene units as the monomer concentration is lowered. In "starved catalyst" conditions, that is, as [M] → 0, *rac*-(EBI)$ZrCl_2$/MAO produces atactic propene oligomers ($\bar{M}_n$ = 1080, mmmm = 9.1%). These effects are the most probable cause for the discordance of literature data on metallocene-catalyzed propene polymerization. Three chain transfer mechanisms have been detected: β-hydrogen transfer to the metal and β-hydrogen transfer to the monomer, both occurring after a *primary* insertion, and β-hydrogen transfer to the monomer after a *secondary* insertion with the exclusive formation of a *cis*-2-butenyl end group.

Introduction

The intense research activity on the polymerization of olefins with metallocene catalysts in both academic and industrial laboratories has added a tremendous amount of detail to the knowledge of the intimate mechanism of active site formation, olefin insertion/elimination reactions, the relationship between catalyst symmetry and polymer microstructure, and the structure/property relationships of the produced polymers. Ewen[2] and Kaminsky[3] showed that the homogeneous catalyst systems composed of Brintzinger's[4] *racemic* [ethylenebis(1-indenyl)]MCl_2 or *racemic* [ethylenebis(4,5,6,7-tetrahydro-1-indenyl)]MCl_2 (M = Ti, Zr, Hf) and methylaluminoxane (MAO) produce isotactic polypropene (iPP) by enantiomorphic site control. The mechanism of isospecific propene polymerization with chiral, C_2-symmetric group 4 metallocene catalysts has been rationalized by Guerra and co-workers[5] and others[6] in terms of a monometallic, cationic, *single-center*[7] catalyst of the type L_2MR^+. Their model, built upon the seminal work of Eisch[8] and Jordan,[9] and experimentally confirmed by several authors,[10] explains the preference for primary monomer insertion, the highly variable stereospecificities obtained with different ligands and the presence of isolated regioinverted units (≈1% secondary insertions) in polypropenes produced with these catalysts.

Although inadequate for the industrial production of iPP when compared with $MgCl_2$-supported Ti-based catalysts,[11,12] the now classic *rac*-[ethylenebis(1-indenyl)]zirconium dichloride (*rac*-(EBI)$ZrCl_2$) (Chart 1) and *rac*-[ethylenebis(4,5,6,7-tetrahydro-1-indenyl)]zirconium dichloride (*rac*-(EBTHI)$ZrCl_2$) precatalysts are often used for comparison when new metallocenes are introduced,[2e,13] and several studies on their polymerization behavior have been reported.[12,14] However, literature data on polymerization activity and degree of regio- and stereospecificity of these prototypical isospecific metallocene catalysts vary in a wide range and make comparisons difficult. Although differences in catalyst activities are readily explained in terms of different experimental conditions, the source of the MAO cocatalyst and purity of the metallocene precatalyst, the scatter of polymer regioregularity, stereoregularity, molecular weight, solubility, and melting point data cannot be explained by the usual differences among different laboratories.

Chart 1

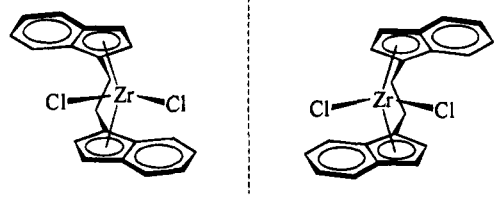

(R,R) (S,S)

1

racemic-EBIZrCl$_2$

Low-pressure propene polymerization in toluene solution is the most common way metallocene catalysts are investigated. In those experiments, propene concentration can vary dramatically, especially when different polymerization temperatures are compared or high productivities are involved (thus approaching the condi-

⊗ Abstract published in *Advance ACS Abstracts,* August 1, 1995.

0024-9297/95/2228-6667$09.00/0

Table 1. Propene Polymerization with 1/MAO in Toluene (50 °C, 1 h)

sample	amt of Zr, μmol	Al/Zr molar ratio	[propene], mol/L	yield, g	$[\eta]$,[a] dL/g	$\bar{M}_v$[b]
1	0.53	8000	10.96 → 10.91	149.7	0.46	36 600
2	0.48	17800	10.89 → 10.64	164.6	0.45	35 600
3	0.48	8000	10.79 → 10.64	66.7	0.44	34 500
4	0.48	7900	4.41	34.2	0.38	28 300
5	0.53	8000	2.84	109.0	0.34	24 300
6	0.55	8200	1.33	34.3	0.33	23 400
7	2.08	2000	1.33	109.3	0.32	22 400
8	2.15	2000	0.85	59.0	0.31	21 500
9	0.56	8000	0.49	10.5	0.29	19 600
10	2.08	2000	0.49	42.0	0.29	19 600
11	1.20	8000	0.4[c]	7.1	0.20	11 900
12	2.08	2000	0.4[c]	4.7	0.16	8 800
13	4.78	8000	→0[d]	0.7	n.d.	liquid[e]

[a] Experimental intrinsic viscosities, THN, 135 °C. [b] Calculated from $[\eta]$ according to $[\eta] = K\bar{M}_v^{\alpha}$ with $K = 1.93 \times 10^{-4}$ and $\alpha = 0.74$. [c] Tests at a nominal 1 bar, but likely under diffusion controlled conditions. [d] Test run in starved catalyst conditions, $[C_3] \rightarrow 0$. [e] $\bar{M}_n = 1080$ from ^{13}C NMR.

tions of diffusion control), but the possible effects of monomer concentration on the behavior of *isospecific* metallocenes have been neglected for a long time, with the exception of Kaminsky's work[14a] which, however, was limited in its scope to propagation rate and molecular weight aspects with the system *rac*-(EBI)$ZrCl_2$/MAO in a relatively narrow monomer concentration range. Very recently, Rieger,[15] Brintzinger,[16] Spaleck,[13f] and ourselves[1] reported the effect of monomer concentration on the molecular weight of iPP produced with different chiral zirconocenes. Brintzinger showed that the molecular weight dependence on monomer concentration can be explained by the competition between monomolecular (β-hydrogen transfer to the metal) and bimolecular (β-hydrogen transfer to the monomer) chain transfer reactions and that the ratio between the two reaction rates strongly depends on the type of cyclopentadienyl ligand. Furthermore, we[1] and others[17] have found that propylene concentration has a strong and unexpected influence on the degree of isotacticity and type of regiomistakes of iPP produced with Brintzinger-type chiral *ansa*-zirconocenes. These findings provide an explanation of the above mentioned discordance of literature data. Despite the large body of literature available on the topic, a set of polymerization results large enough to allow a detailed kinetic analysis is not yet available. In this paper we report the details of our investigation on propene polymerization with the moderately isospecific *rac*-(EBI)$ZrCl_2$/MAO (**1**/MAO) catalyst.

Results and Discussion

Aiming at evaluating the effect of the different Cp ligand structures on iPP molecular weight, we started our investigation several years ago by obtaining sound molecular weight data for iPP produced from the *rac*-(EBI)$ZrCl_2$/MAO catalyst (**1**/MAO) in different polymerization conditions. A general observation among the different groups working in this field was that the polymerization behavior of a given metallocene catalyst was very dependent on the experimental conditions, much more so than for heterogeneous catalysts. In particular, we found at the beginning of our investigation that low-pressure polymerizations in toluene solution produced a much lower molecular weight iPP than those in liquid monomer, with most of the metallocenes investigated. The increase of iPP molecular weight with propene concentration had been reported by Kaminsky, who explored the range 0.6–5 M at 35 °C with **1**/MAO,[14a] and then obtained propene oligomers with a related catalyst at 50 °C and very low monomer concentration.[18] Therefore, to investigate the effect of propene concentration on the chain transfer reactions with this catalyst, we polymerized propene with **1**/MAO at 50 °C in toluene/propene mixtures at monomer concentrations varying from ca. 0 to ca. 11 mol/L. We had chosen a polymerization temperature of 50 °C as the best compromise between ease of lab-scale batch polymerization procedure and the practical (from the standpoint of industrial production) range of polymerization temperatures. For some values of propene concentration, two levels of the Al/Zr ratio were also investigated. The results from iPP samples are presented in Tables 1 and 2. Monomer concentrations were calculated as described in the Experimental Section. In Table 1 a concentration range is shown for polymerization tests in liquid monomer. The two values correspond to the initial (higher value, $t_p = 0$ min) and final (lower value, $t_p = 60$ min) concentrations due to partial monomer consumption.

Our experimental conditions do not allow detailed kinetic measurements such as propagation rates, and no final relationship between propagation rate and monomer concentration could be established from the observed productivities. Polymerization tests repeated after long times, while showing different catalyst productivities due to the different purities of the fluids (monomer, toluene, nitrogen) always produced polymer samples with excellent reproducibility in their molecular properties.

Table 2. DSC and ^{13}C NMR Characterization of iPP Samples

			tacticity[b]				regioinversions, %[c]			
sample	average [propene], mol/L	T_m,[a] °C	b	m	mm	mmmm	2,1 E	2,1 T	1,3	2,1/1,3
1	10.93	135	0.9710	94.4	91.6	86.3	0.3_6	0.2_0	traces	
2	10.77	133	0.9673	93.7	90.5	84.7	0.3_7	0.1_7	$\leq 0.0_4$	
3	10.72	136	0.9725	94.7	92.0	87.0	0.3_5	0.1_9	$\leq 0.0_4$	
4	4.41	133	0.9705	94.3	91.4	86.1	0.3_7	0.1_7	0.0_4	$13._5$
5	2.84	131	0.9707	94.3	91.5	86.2	0.4_3	0.2_2	0.0_7	$8._0$
6	1.33	131	0.9673	93.7	90.5	84.7	0.3_5	0.1_7	0.1_4	3.7_5
7	1.33	131	0.9682	93.9	90.8	85.1	0.3_4	0.1_7	0.1_5	3.7_7
8	0.85	128	0.9621	92.7	89.1	82.4	0.2_6	0.1_5	0.2_4	2.1_5
9	0.49	125	0.9557	91.5	87.3	79.7	0.2_5	0.1_3	0.2_8	1.3_8
10	0.49	123	0.9551	91.4	87.1	79.5	0.2_3	0.0_9	0.2_9	1.3_3
11	0.4	113	0.9267	86.4	79.6	68.3	0.2_1	0.1_1	0.3_9	0.7_5
12	0.4	86	0.8863	79.8	69.8	54.7			0.5_8	
13	→0	liquid	0.6057	52.2	28.3	9.11			0.5_4	

[a] Melting points determined from the second melting; see experimental part. [b] Determined by assuming the enantiomorphic site model; see text. [c] Determined as described in the text.

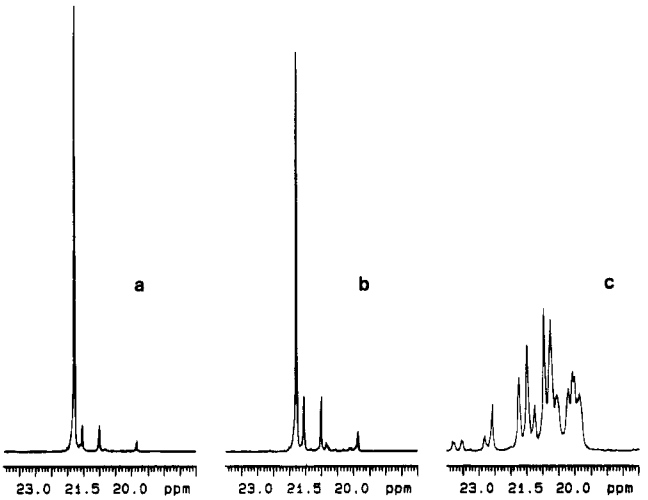

Figure 1. ^{13}C NMR pentad region of samples **1** (a), **11** (b), and **13** (c).

Scheme 1

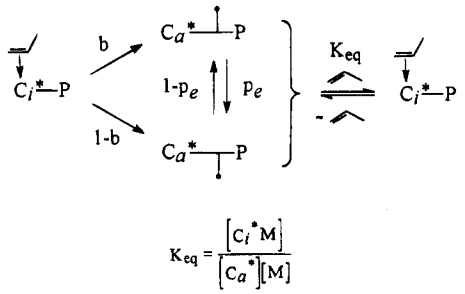

$$K_{eq} = \frac{[C_i^*M]}{[C_a^*][M]}$$

Isotacticity. The most unexpected effect of monomer concentration is the relatively strong variation of the polymer microstructure, as both isotacticity and regioregularity are affected. The ^{13}C NMR characterization of our iPP samples is reported in Table 2.

As previously reported[1] and in accordance with the results of Busico,[17] we observe that isotacticity (% mmmm) decreases from 87 to 54.7% by decreasing the monomer concentration from 11 to 0.4 mol/L. While a tacticity dependence on monomer concentration has been observed and explained by Ewen in the case of syndiospecific propene polymerization,[19] and more recently by Rieger[15] (who found an *inverse* dependence of isotacticity on monomer concentration for a different class of metallocene catalysts), in our case this effect is unexpected. As a matter of fact, as far as enantioface selectivity is concerned, C_2-symmetric chiral metallocenes should not sense on what side, and how often, a monomer approaches the metal center.[5,20] To see how far this loss of enantioface selectivity would go by decreasing monomer concentration, we also ran a polymerization experiment under "starved catalyst" conditions, such as [M] → 0 (sample 13). The resulting oligomers were *fully atactic* (see Table 2). The ^{13}C NMR pentad region for samples **1**, **11**, and **13** is reported in Figure 1.

To explain the loss of stereospecificity with the decrease in monomer concentration, we postulate an equilibrium between an isospecific site C_i*M having a coordinated monomer (in analogy to the model we propose to account for the molecular weight behavior, vide infra) and an aspecific one C_a* without coordinated monomer (Scheme 1):

It is apparent from Scheme 1 that C_a*, not having a coordinated monomer molecule, can not generate m,r dyads by monomer insertion. As a consequence, C_a* must be able to racemize the chiral carbon of the last inserted unit; that is, as also pointed out by the Busico and Cipullo,[17] and experimentally proven by Brintzinger and Leclerc by polymerizing (*Z*)- and (*E*)-propene-*1-d*,[21] C_a* is an epimerization catalyst.[22]

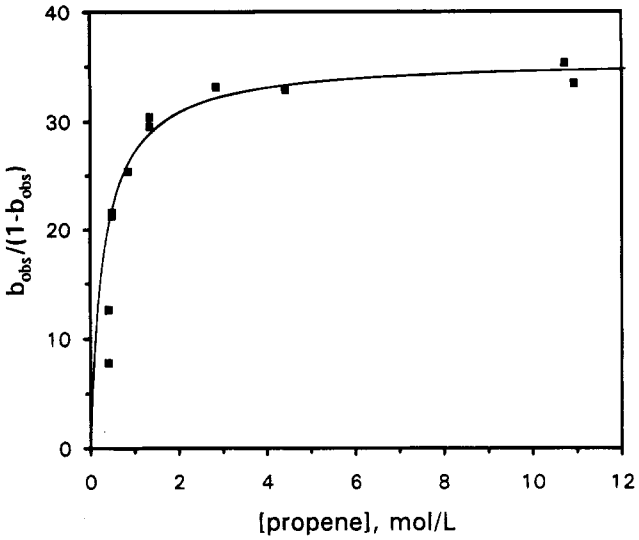

Figure 2. $b_{obs}/(1 - b_{obs})$ versus [M]: (■) experimental values, (—) best fit with eq 1.

In Scheme 1, p_e is the probability of epimerization (racemization) of the last stereogenic methine, b is the probability of a correct enantioface insertion (*re* at an *R,R* center and *si* at an *S,S* center), and the sites C_a* and C_i*M are related by

$$[C_i^*M] = [C_a^*]K_{eq}[M]$$

Hence, assuming $p_e = 1 - p_e = 0.5$ (i.e. assuming C_a* to lose *any* enantioface selectivity in the absence of coordinated monomer, as inferred from the microstructure of sample **13**), and introducing the molar fractions $X_i = C_i^*/C^*$ for propagating centers and $X_a = C_a^*/C^*$ for epimerization centers, one obtains

$$\frac{b_{obs}}{1 - b_{obs}} = \frac{b(1-p_e)X_a + (1-b)(1-p_e)X_a + bX_aK_{eq}[M]}{(1-b)p_eX_a + bp_eX_a + (1-b)X_aK_{eq}[M]} = \frac{(1-p_e)X_a + bX_aK_{eq}[M]}{p_eX_a + (1-b)X_aK_{eq}[M]} = \frac{0.5 + bK_{eq}[M]}{0.5 + (1-b)K_{eq}[M]} \quad (1)$$

where b_{obs} and $(1 - b_{obs})$ are the *observed* concentrations, at a given [propene], of correct and wrong propene units, respectively, as obtained by the ^{13}C NMR data (see Experimental Section) and K_{eq} is as defined in Scheme 1.

The experimental $b_{obs}/(1 - b_{obs})$ data and the best fit obtained from eq 1 are reported in Figure 2. The best fit of $b_{obs}/(1 - b_{obs})$ for samples **1**–**10** with eq 1 gives K_{eq} = 56.7 L/mol and b = 0.9727, where b is the maximum—or inherent—enantioface selectivity of the isospecific catalyst $\mathbf{1}^+$ for propene at T_p = 50 °C, corresponding to m = 0.9470, in excellent agreement with the experimental values of 0.944 and 0.947 observed in liquid monomer (samples **1** and **3**, Table 2).

The consequence of the above results is that the active center needs a coordinated monomer molecule in order to retain its stereospecificity.

Scheme 2. Sequences of Propylene Insertions at a [(*R*,*R*)(EBI)Zr-P]$^+$ Center Leading to Isolated Secondary Units[5e]

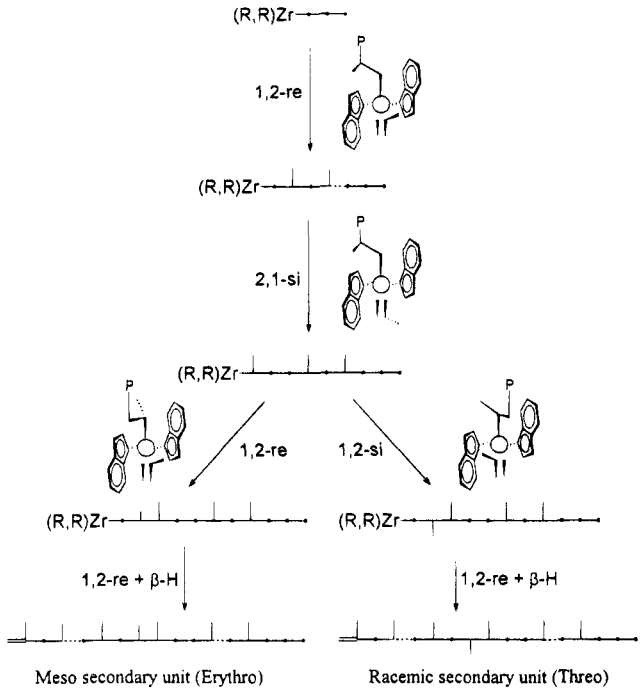

Chart 2. Trans-Planar Representation of Erythro (Meso) and Threo (Racemic) Secondary Units[a]

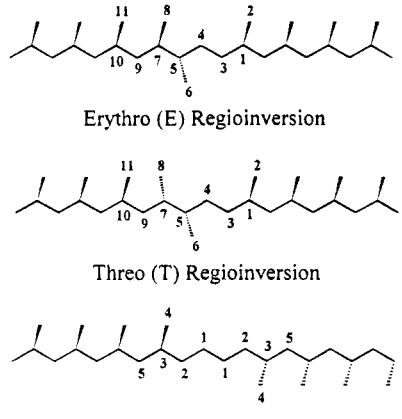

[a] The saturated (*n*-propyl) end group lays on the right of the chain segment; the unsaturated one (vinylidene), on the left. The chain segment containing a 1,3-unit is also shown.

Regioregularity. The most characteristic feature of the microstructure of zirconocene- and hafnocene-produced iPP is the presence of isolated secondary (2,1 insertions) propene units in the isotactic sequences of primary propene insertions and of the so-called 1,3 propene insertion.[12] The relative amounts of these regiodefects are highly dependent on the metallocene and the polymerization conditions employed. It is worth noting here that an isolated 2,1 unit gives a direction to the polymer chain, hence making it possible to define the monomer temporal sequencing in the immediate surroundings of such an isolated secondary unit (Scheme 2 and Chart 2). The two types of 2,1 regioinversions, erythro (E) and threo (T),[23] observed in iPP prepared with **1**/MAO, have been unambiguously assigned by Mizuno et al. through a detailed $^{13}C-^{1}H$ 2D NMR analysis[24] and rationalized by Guerra and co-workers.[5e]

As shown in Table 2, these secondary units are more likely to isomerize into 1,3 propene units when the monomer concentration is lowered while both their ratio (E/T $\approx$ 2) and the overall percentage ($\approx$0.7%) of regio-inverted units including 1,3 remains approximately constant. Hence, in first approximation we can assume that regiospecificity is independent from monomer concentration. The 2,1 $\rightarrow$ 1,3 transformation can be rationalized in terms of the polymerization rates: the higher the time between two insertions, the higher is the chance of the last (secondary) inserted unit to undergo isomerization.

Scheme 3

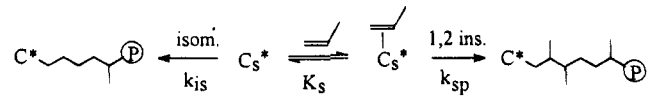

Proton and carbon NMR of samples **11**–**13** showed that, as expected, the only detectable olefin end groups are of the vinylidene type. No internal or CH_2=$CHCH_2$-CH_2– double bonds could be seen, showing that hydrogen transfer after a 2,1 or 1,3 insertion is highly disfavored at low monomer concentrations, even if the lifetime of a secondary growing chain is expected to be much longer than that of a primary chain.[14b,d] The above observation is in favor of a nondissociative mechanism for the 2,1 $\rightarrow$ 1,3 transformation.[12a,b,25]

The competition between the two reaction pathways (secondary chain end isomerization with formation of a 1,3 propene unit versus primary insertion onto the metal secondary chain end *site*[7] C_s*) can be described, in the same way as in the case of stereospecificity, by eq 2 and is shown in Scheme 3. R_{sp} and k_{sp} are the rate and constant of insertion of a primary unit onto a secondary chain end, R_{is} and k_{is} are the rate and constant of secondary chain end isomerization and C_s* and C_s*M are the active centers having a secondary chain end and none or one coordinated monomer molecules, respectively, and are correlated by the equilibrium constant $K_s = [C_s*M]/[C_s*][M]$:

$$\frac{[2,1]}{[1,3]} = \frac{R_{sp}}{R_{is}} = \frac{k_{sp}[C_s*M]}{k_{is}[C_s*]} = \frac{k_{sp}K_s[M]}{k_{is}} \qquad (2)$$

The amount of 2,1 and 1,3 units can be calculated from the methylene carbons according to[12d] % 2,1 = 100·$(0.5S_{\alpha\beta})/(S_{\alpha\alpha} + S_{\alpha\beta} + S_{\alpha\delta})$ and % 1,3 = $100(0.5S_{\alpha\delta})/(S_{\alpha\alpha} + S_{\alpha\beta} + S_{\alpha\delta})$ where $S_{\alpha\beta}$ is better evaluated from the peak areas of the E_9 and T_9 isolated $S_{\alpha\alpha}$ methylenes at 42.2 and 43.2 ppm, and $S_{\alpha\delta}$ is the peak area of methylene H_2 at 37.35 ppm (carbons labeled as shown in Chart 2, chemical shifts referenced to the mmmm pentad at 21.8 ppm).

We use the relationships % 2,1 E = $100E_9$/total CH_2, % 2,1 T = $100T_9$/total CH_2, and % 1,3 = $50H_2$/total CH_2 where the total methylene area is given by total CH_2 = CH_2(main) + $3E_9$ + $3T_9$ + H_2. Given the low amount of regioinversions found in the samples, some error is introduced when the $S_{\alpha\beta}$ and $S_{\alpha\delta}$ peaks are compared to the main $S_{\alpha\alpha}$ methylene peak. To minimize errors, the 2,1/1,3 ratio is calculated directly as 2,1/1,3 = $2(E_9 + T_9)/H_2$.

The experimental [2,1]/[1,3] ratios for samples **4**–**11** depend linearly on propene concentration with a correlation parameter R = 0.998, from which we obtain $K_s k_{sp}/k_{is}$ = 3. In samples **1**–**3** the amount of 1,3 units is too low (although detectable) for accurate evaluation. A similar dependence of the [2,1]/[1,3] ratio on [propene] for **1**/MAO at 60 °C has been reported by Busico et al.

Scheme 4[a]

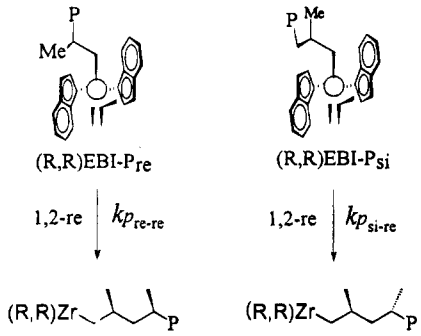

[a] $k_{p_{rere}}$ and $k_{p_{sire}}$ are the rate constants of primary *re* insertion onto (*R,R*)EBI$^+$ centers (C*$_{re}$ ≡ (R,R)EBI-P$_{re}$ and C*$_{si}$ ≡ (*R,R*)EBI-P$_{si}$) bearing primary *re* and primary *si* chain end units, respectively. In the case of (*R,R*)EBI$^+$, $k_{p_{rere}} > k_{p_{sire}}$.

Propagation Rate. It has been shown that propene insertion at sites bearing primary chain ends is faster than at sites bearing secondary chain ends.[17c,26] It is also intuitive[7,17] that propagation rates should be different at the two diastereomeric sites of **1**$^+$ bearing *primary* chain ends with the last methine of opposite chirality, C*$_{re}$ and C*$_{si}$ (shown in Scheme 4 for (*R,R*) centers). Note that we assume the two primary sites to have the same (or very similar) enantioselectivity, as we could not detect any penultimate monomer unit effect.

Without loss of generality, the following discussion is based on (*R,R*) centers, for which we assume the propagation rate constant for correct (*re* face) insertion onto an *re* chain end to be higher than the propagation rate constant for correct (*re* face) insertion onto an *si* chain end,[17] that is $k_{rere} > k_{sire}$ (Scheme 4).

Although the total number of active centers decreases with time (observed decay profiles were very similar to those already reported for **1**/MAO[14c,e] and related systems[16]), at any instant, at a given polymerization temperature and monomer concentration, the molar fraction X_j (with respect to the total concentration of active centers[7] C*) of each different site[7] *j* is constant. The amount of total secondary insertions is constant with respect to [propene]. Let us consider the molar fractions X_{re} and X_{si} of the two different primary active sites C*$_{re}$ and C*$_{si}$. Because of epimerization, X_{re} decreases and X_{si} increases as [propene] decreases, and their values are given by (see eq 1)

$$[C^*_{re}] = X_{re}[C^*] = b_{obs}[C^*] = [C^*](0.5 + bK_{eq}[M])/(1 + K_{eq}[M])$$

and

$$[C^*_{si}] = X_{si}[C^*] = (1 - b_{obs})[C^*] = [C^*](0.5 + (1 - b)K_{eq}[M])/(1 + K_{eq}[M]) \quad (3)$$

Hence, assuming the concentration of metal hydride species to be negligible in the range 0.49−11 mol/L and all rate constants to be independent from chain length and taking into account the above relationships and the four possible elementary steps of primary insertions resulting from *re*, *si* olefin insertions on the two different sites C*$_{re}$ and C*$_{si}$, we can write the overall rate of *primary* propagation on *primary* chain end sites as:

$$\begin{aligned} R_p &= R_{rere} + R_{resi} + R_{sisi} + R_{sire} \\ &= (k_{rere} + k_{resi})[C^*_{re}][M] + (k_{sisi} + k_{sire})[C^*_{si}][M] \\ &= \{(k_{rere} + k_{resi})X_{re} + (k_{sisi} + k_{sire})X_{si}\}[C^*][M] \\ &= \{(k_{rere} + k_{resi})(0.5 + bK_{eq}[M])/(1 + K_{eq}[M]) + (k_{sisi} + k_{sire})(0.5 + (1 - b)K_{eq}[M])/(1 + K_{eq}[M])\}[C^*][M] \\ &= \{[0.5(k_{rere} + k_{resi}) + 0.5(k_{sisi} + k_{sire})]/(1 + K_{eq}[M])\}[C^*][M] + \{[(k_{rere} + k_{resi})bK_{eq} + (k_{sisi} + k_{sire})(1 - b)K_{eq}]/(1 + K_{eq}[M])\}[C^*][M]^2 \quad (4) \end{aligned}$$

Equation 4 reduces to $R_p \approx [0.5(k_{rere} + k_{resi}) + 0.5(k_{sisi} + k_{sire})][C^*][M]$ for [M] → 0, and to $R_p \approx [(k_{rere} + k_{resi})b + (k_{sisi} + k_{sire})(1 - b)][C^*][M]$ for [M] → maximum.

It appears that two enantioselective active sites, whose relative mole fractions are a function of monomer concentration and which have the same enantioface selectivity but different rate constants for insertion, generate a propagation rate law with an apparently exponential dependence on [propene].

A law of propagation rate for stereospecific catalysts of the type described above can explain the experimentally observed propagation rates with dependence on [propene] having *apparent* order between 1 and 2.[19,27]

All other insertion reactions at the different sites[7] of **1** (secondary insertion on primary chain ends and *re* and *si* primary insertion onto secondary chain ends; see Scheme 2) will contribute to either term of eq 4, without modifying its general form.

Note that aspecific catalysts, for which $b \approx (1 - b) \approx 0.5$, will have $R_p \approx [0.5(k_{rere} + k_{resi}) + 0.5(k_{sisi} + k_{sire})][C^*][M]$, that is the usual linear dependence of R_p on monomer concentration, in all ranges of [M].

Molecular Weight. As expected, iPP molecular weight is monomer concentration dependent: iPP with intrinsic viscosities [η] (measured in tetrahydronaphthalene at 135 °C) ranging from 0.16 to 0.46 dL/g ($\bar{M}_v$'s from 8800 to 36 600) were obtained (see samples **1**−**12**, Table 1) at monomer concentrations between 0.4 and 11 mol/L (1−20.5 bar). Sample **13**, prepared at [M] → 0, consisted of liquid oligomers with $\bar{M}_n$ of 1080, as determined by ^{13}C NMR. It is worth noting that we have confirmed the change of $\bar{M}$ with [propene] through three different independent techniques, that is viscosimetry, NMR, and GPC. In all cases, the dependence of molecular weight on monomer concentration *does not* follow a linear relationship in the whole range investigated, being much higher below about 1 mol/L (see below).

The shapes and the narrowness of the molecular weight distributions observed ($\bar{M}_w/\bar{M}_n \approx 2$) are the signature of a Schulz−Flory distribution for a single-center[7] catalyst, confirming previous results.[12d,28,29] Larger values reported in the literature are probably the result of poor temperature and/or monomer feed control during polymerization and are not due to the presence of multiple active centers. The homogeneity of our samples was confirmed by solvent extraction of sample **8**: no polymer soluble in Et_2O (atactic) could be obtained, while 95% of it was soluble in refluxing *n*-hexane and 5% in refluxing *n*-heptane (Kumagawa extraction, 8 h).

The molecular weight depends on the ratio between the overall propagation rate and total chain transfer rates ($\bar{P}_n = \sum R_p/\sum R_t$) and is in general independent from

Scheme 5. Chain Transfer to Aluminum: $R_t = k_{tAl}[C^*][Al]$

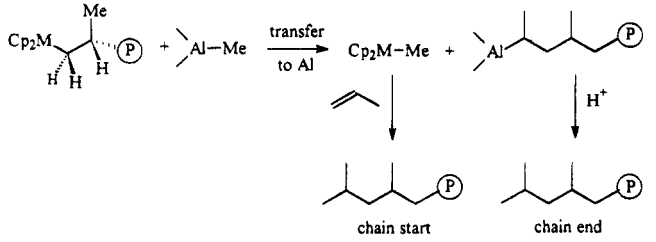

Scheme 6. Monomolecular Hydrogen Transfer (β-H Transfer to the Metal): $R_t = k_{tMet}[C^*]$

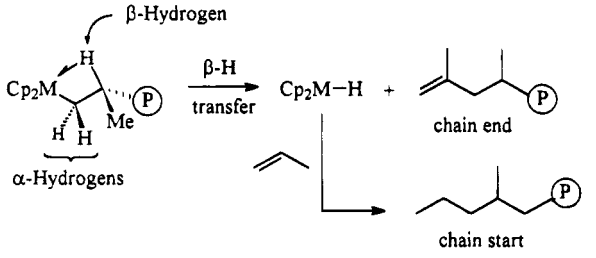

Scheme 7. Bimolecular Hydrogen Transfer (β-H Transfer to the Monomer): $R_t = k_{tMet}[C^*][M]$

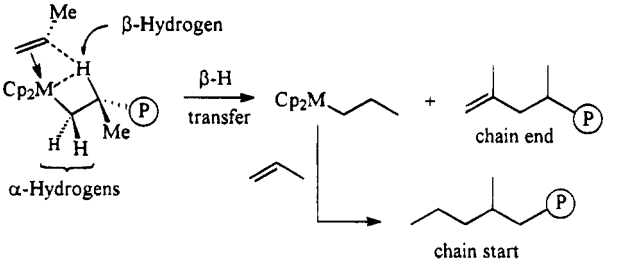

Scheme 8. β-H Transfer to the Monomer after a Secondary Insertion at (R,R)(EBI)Zr^{+a}

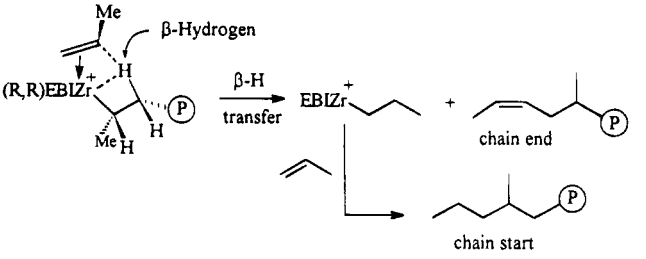

[a] The *cis*-2-butenyl end group is more likely to form than *trans*-2-butenyl because of steric interactions.

the number of active centers, that is independent from the observed catalyst productivity.

Two main types of chain transfer processes have been observed with chiral metallocene catalysts: chain transfer via β-H elimination (after a primary or secondary insertion) and chain transfer to the aluminum cocatalyst. In low molecular weight polypropylenes, both types can be easily recognized by the structure of unsaturated and saturated end groups, as observable by ^{1}H and ^{13}C NMR spectra.

The effect of methylaluminoxane type and the Al/Zr ratio (in the range investigated) for **1**/MAO is mainly, if not only, on catalyst activity, as already observed in several cases (compare samples **1** with **2** and **3**, **6** with **7**, and **9** with **10**). In particular we did not observe (based on the absence of isobutyl end groups in the ^{13}C NMR spectra of the polymers (see Scheme 5) and molecular weight invariance with different Al/Zr ratios) any chain transfer to aluminum,[30] with the exception of samples **12** and **13**, for which transfer to aluminum was 10 and 50%, respectively. In these two cases, for which insertion rates were very low, chain transfer to aluminum becomes a competitive process.

End-group analysis on the polymers produced from a number of different metallocene catalysts has shown that chain transfer mostly occurs via β-H elimination after a primary insertion,[12b,c,27,28] with the formation of *n*-propyl and vinylidene end groups. Chain transfer via β-H elimination after a *primary* insertion can be monomolecular (hydride transfer to the metal, zero order in monomer concentration, Scheme 6) or bimolecular (hydride transfer to the monomer, first order in monomer concentration, Scheme 7); both processes will produce identical end groups (*n*-propyl and vinylidene) and thus are indistinguishable by NMR analysis.

For a given metallocene one has to establish whether chain transfer via β-H elimination is monomolecular (β-hydrogen transfer to the metal) or bimolecular (β-hydrogen transfer to the monomer) only, as some authors have suggested.[10d,14d,31] Kaminsky's results[14a] with **1**/MAO indicate that both rate of propagation and molecular weight increase linearly with monomer concentration (range 0.6–5 M at 35 °C), a behavior diagnostic of monomolecular chain transfer, but the concentration range was too narrow to allow any final conclusions. The presence of a dependence of molecular weight on [propene] rules out the simplified picture of both propagation and chain transfer being first order in [propene] in the case of **1**/MAO.[17c]

The ratio between the rates of hydrogen transfer to the metal ($R_{tMet} = k_{tMet}[C^*]$) and hydrogen transfer to the monomer ($R_{tMon} = k_{tMon}[C^*][M]$) can be estimated, at a given polymerization temperature, by evaluating the molecular weight dependence on [propene]. The recent report by Brintzinger[16] indicates that, at least for the investigated silane-bridged zirconocenes, both mechanisms compete in lowering iPP molecular weight (eq 5).

$$\bar{P}_n = \frac{k_p[C^*][M]}{k_{tMet}[C^*] + k_{tMon}[C^*][M]} \quad (5)$$

In the present investigation we have found that, at higher monomer concentrations, also 2-butenyl end groups (ca. 30% of total unsaturated end groups) become detectable in the olefin region of the polymers ^{1}H NMR spectra (multiplet at 5.35–5.5 ppm). Vinylidene end groups (from transfer after primary insertion) are always predominant and are the only unsaturations detectable in the lower molecular weight samples **11**–**13**. 2-Butenyl end groups have been previously observed in iPP made with *rac*-[ethylenebis(tetrahydroindenyl)]$ZrCl_2$/MAO[32] and **1**/MAO[14b] at lower polymerization temperatures. Their presence at high monomer concentrations indicates that also β-H transfer from the last chain methylene to the coordinated monomer after a *secondary* insertion is an accessible chain transfer pathway for these systems (Scheme 8).

Chain transfer via β-H elimination after a *secondary* insertion is clearly a methylene hydride transfer to the monomer. β-H elimination of a methyl hydrogen is not observed and is unlikely due to steric hindrance (in the conformation leading to chain transfer, the growing chain would be forced toward one of the phenyl rings of the EBI ligand).

The viscosimetric molecular weight dependence on monomer concentration for **1**/MAO at 50 °C is shown

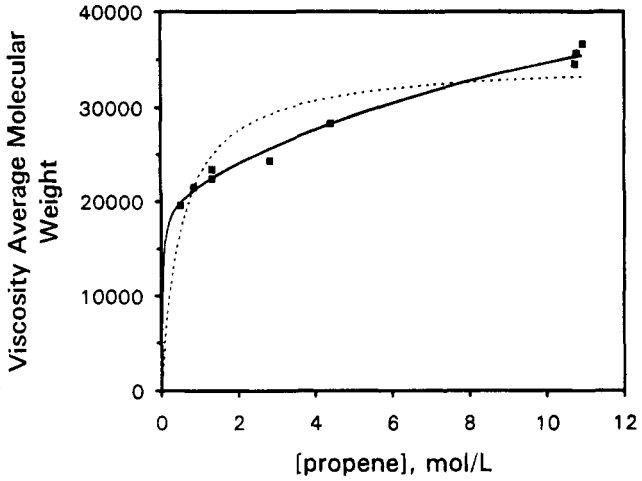

Figure 3. (■) Experimental average viscosimetric molecular weights versus [propene]: (- - -) best fit with eq 5, (—) best fit with eq 9.

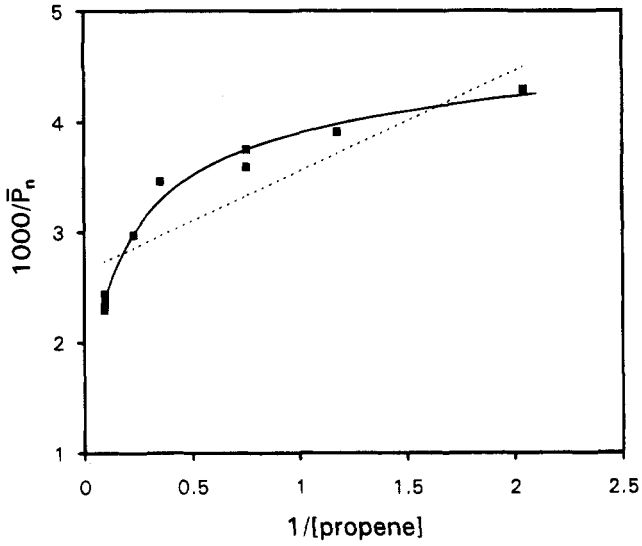

Figure 4. (■) Reciprocal of number average degrees of polymerization ($1/\bar{P}_n$) versus 1/[propene]: (- - -) best fit with eq 6, (—) best fit with the reciprocal of eq 9 [$1/\bar{P}_n = (k'_{t_0}/[M]^2 + k'_{t_1}/[M] + k'_{t_2})/(k'_{p_1}/[M] + k'_{p_2})$].

in Figure 3, together with the function defined by eq 5. Our molecular weight values, with the change in slope at 1 mol/L, confirms that also for **1**/MAO there are at least two chain transfer mechanisms with a different order on [propene]. However, our data obey the linear form of eq 5[16]

$$\frac{1}{\bar{P}_n} = \frac{k_{tMon}}{k_p} + \frac{k_{tMet}}{k_p}\frac{1}{[M]} \qquad (6)$$

only in the range 0.49–2.84 mol/L (1.2–4 bar) while a deviation from linearity is observed above 4 bar (Figure 4). This indicates that the model described by eq 5 is too simplified for propene polymerization with **1**/MAO.

Our molecular weight data provide an experimental confirmation for the hypothesis of propagation rate having the form $R_p = k'_{p_1}[M] + k'_{p_2}[M]^2$. In our conditions, in the [propene] range 0.49–11 mol/L, in which transfer to aluminum is negligible, and using the same assumptions as for the derivation of the propagation law, an expression for $\bar{P}_n$ can be derived which matches the experimentally observed molecular weights far better than eq 5.

As discussed above, chain transfer via β-hydrogen transfer from a primary chain end can be zero or first order in [propene], and in addition k_t could be expected to be different for the two different primary sites, C^*_{re} and C^*_{si}. Both these sites can have (C*M) or not have (C*) a coordinated propene molecule (Scheme 9).

Scheme 9

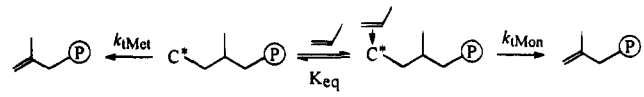

Here the two species are the same invoked to explain the change in stereoselectivity, and again $[C^*M] = K_{eq}[C^*][M]$. Hence, $R_{\beta\text{-H,primary}} = k_{tMet}[C^*] + k_{tMon}K_{eq}[C^*][M]$.

Hence, the rate of chain transfer from a primary chain end (at an (*R*,*R*) center) is

$$R_t = k_{tMet,re}[C^*_{re}] + k_{tMet,si}[C^*_{si}] + k_{tMon,re}K_{eq}[C^*_{re}][M] + k_{tMon,si}K_{eq}[C^*_{si}][M] \qquad (7)$$

From eqs 3 and 7, one obtains

$$R_{t,primary} = k_{tMet,re}[C^*_{re}] + k_{tMet,si}[C^*_{si}] + k_{tMon,re}[C^*_{re}][M] + k_{tMon,si}[C^*_{si}][M] = \{k_{tMet,re}(0.5 + bK_{eq}[M])/(1 + K_{eq}[M]) + k_{tMet,si}(0.5 + (1 - b)K_{eq}[M])/(1 + K_{eq}[M])\}[C^*] + \{k_{tMon,re}K_{eq}(0.5 + bK_{eq}[M])/(1 + K_{eq}[M])[M] + k_{tMon,si}K_{eq}(0.5 + (1 - b)K_{eq}[M])/(1 + K_{eq}[M])\}[C^*][M] = 0.5[C^*](k_{tMet,re} + k_{tMet,si})/(1 + K_{eq}[M]) + [C^*][M]\{k_{tMet,re}bK_{eq} + k_{tMet,si}(1 - b)K_{eq} + 0.5k_{tMon,re}K_{eq} + 0.5k_{tMon,si}K_{eq}\}/(1 + K_{eq}[M]) + [C^*][M]^2\{k_{tMon,re}bK_{eq}^2 + k_{tMon,si}(1 - b)K_{eq}^2\}/(1 + K_{eq}[M]) \qquad (8)$$

where the subscripts *re*, *si* refer to the chirality of the last inserted unit.

Hence, the overall law for $\bar{P}_n$ has the form

$$\bar{P}_n = \frac{k'_{P_1}[M] + k'_{p_2}[M]^2}{k'_{tMet} + k'_{t_1}[M] + k'_{t_2}[M]^2} \qquad (9)$$

where k'' are apparent rate constants, partially defined in eqs 4 and 8.

In Figure 3 the function defined by eq 9, with the approximation $\bar{M}_v \approx \bar{M}_w = 2\bar{M}_n$, is shown along with eq 5 and the experimental viscosimetric molecular weight data, showing the closer fit obtained in our case for samples **1**–**10** obtained at [propene] in the range 0.49–10.93 mol/L, where monomer concentrations could be evaluated with good confidence. In Figure 4 we show the $1/\bar{P}_n$ versus 1/[M] plots for the experimental data in the same concentration range, for eq 6 (the linear form of eq 5), and for our model, the reciprocal of eq 9. (The three tests at lower concentrations, samples **11**–**13**, were run under increasingly diffusion-controlled conditions; see Experimental Section.) The better fit provided by our model at the higher concentrations is clearly observable.

Conclusions

The evaluation of the effect of monomer concentration on the fine details of polypropene structure (molecular weight, isotacticity, and type of regioinversions) has proven to be a powerful tool to probe the mechanisms of chain growth and transfer.

We confirm that the molecular architecture of isotactic polypropenes obtained from the chiral isospecific *rac*-(EBI)$ZrCl_2$ is heavily dependent on monomer concentration. This dependence, which appears to be a general one for the present class of catalysts,[17] can in part explain the discordance of literature data on the subject. We also confirm that 1,3 propene isomerization–insertion occurs also with *rac*-(EBI)$ZrCl_2$/MAO.

The effect of monomer concentration on molecular weight has been fully investigated. A new propagation law, which explains the observed molecular weight dependence on propene concentration, has been proposed. Chain transfer after a primary insertion is facile, and as already observed for other chiral zirconocenes,[16] it occurs through two different mechanisms, β-H transfer to the metal and β-H transfer to the monomer. Chain transfer after a secondary insertion is negligible at low monomer concentrations but becomes visible above ca. 0.8 mol/L. From our results, it appears that the active center needs a coordinated monomer molecule in order to retain its stereospecificity.

In light of the results discussed above, which have been found independently in two different laboratories, it appears that literature reports on the effect of polymerization conditions (such as temperature, Al/Zr ratios, cocatalyst, and solvent type) on chiral metallocene catalyst performance (activity, stereo- and regioregularity, propagation/transfer rates), unless obtained in liquid propene, should be taken with some precaution. As a matter of fact, we have reinvestigated the influence of polymerization temperature *in liquid monomer* with **1**/MAO and obtained results that differ considerably from previous reports.[12h,14a] We found that the isotacticity of polypropenes from **1**/MAO is much less dependent on T_p than previously reported:[12h] in liquid monomer, and in the 20–70 °C polymerization temperature range, the percent mmmm, molecular weight, and melting temperature of iPP all decrease *linearly* with increasing T_p, and no abrupt change of these properties is observed at any temperature.

Preliminary polymerization results and polymer characterization give a $\Delta E^{\ddagger}$ of 3.3 kcal/mol for the enantioface selectivity of **1**, which is only moderately isospecific. This value is intermediate between that of enantiomorphic site control of highly isospecific Ti catalysts (4.8 kcal/mol)[33] and that of chain end control (ca. 2 kcal/mol).[33,34]

Chain transfer via β-hydrogen transfer to the monomer after a *secondary* insertion is observed in all samples prepared at the different T_p's, suggesting that C^*_s sites are less inert than previously suggested.[17c] Furthermore, the fraction of 2-butenyl end groups seems, within experimental error, independent of T_p, suggesting that β-hydrogen transfer to the monomer after a secondary insertion has a low energy of activation.

Total secondary insertions increase by increasing T_p, from ca. 0.4% at 20 °C to ca. 0.7% at 70 °C). We are currently investigating the dependence of polypropene molecular properties on polymerization temperature for a number of different chiral zirconocenes.

The rate of epimerization, which has a direct influence on the rate of polymerization, is clearly dependent on ligand structure,[17b] whether it is due to reversible β-hydrogen elimination or to some other processes. The use of zirconocene catalysts which effectively inhibit β-H transfer after a primary insertion even at low [propene] will help elucidate this point. We are investigating such a system and will report the results in the future.

Experimental Section

General Procedures. All operations were performed under nitrogen by using conventional Schlenk-line techniques. Hydrocarbon solvents were distilled from $AliBu_3$ and stored under nitrogen. The typical residual water content was 2 ppm. Polymerization grade propene (containing ca. 5% propane) was received directly from Montell Ferrara plant. *rac*-[Ethylenebis(1-indenyl)]$ZrCl_2$ (*rac*-(EBI)$ZrCl_2$) was prepared according to Collins[35] and purified by CH_2Cl_2 extraction.[36] MAO (Witco, 30% w/w in toluene) was treated as previously recommended[30d] in order to remove most of the unreacted TMA. The isomeric and chemical purities of all compounds were confirmed by ^1H NMR (200 MHz, $CDCl_3$, signal-to-noise ratio 200).

Polymerizations. Polymerization experiments were carried out in either a 1 L Büchi glass autoclave (solution polymerizations with 400 mL of toluene and continuous monomer feed) or a 2 L stainless-steel autoclave (liquid monomer polymerizations) at constant pressure for 1 h. The polymerization temperature was kept within ±1 °C. Nitrogen and propane were eliminated by purging the system for several minutes. Stirring was kept at 800 rpm by means of a three-blade propeller. Samples **11**–**13** were prepared in a 500 mL flask thermostated at 50 °C by means of an external bath with a two-coil heating–cooling system and with previously monomer-saturated solvent (400 mL), rapid stirring (samples **11**–**12**) or adding **1**/MAO to toluene *before* adding the monomer and with slow stirring (sample 13).

Metallocene and MAO were precontacted for 10 min in toluene solution (10 mL) and then added to the monomer/solvent mixture at 48 °C. The polymerizations were quenched with CH_3OH; the polymers were isolated by distilling off the solvents under reduced pressure and dried at 50 °C in vacuo overnight.

Polymer Analysis. Intrinsic viscosities were measured in tetrahydronaphthalene at 135 °C, and converted into average viscosimetric molecular weights using the Mark–Houwink equation for iPP with $\alpha = 0.74$ and $K = 1.93 \times 10^{-4}$.[37]

Calorimetric measurements were obtained on a Perkin-Elmer DSC-7 thermal analyzer calibrated with indium and tin standards, using 4–5 mg samples. The thermograms were recorded at a heating rate of 10 °C/min between 50 and 200 °C. In order to obtain the same thermal history, the polymer samples were kept at 200 °C for a time sufficient to melt all the crystallites that would influence the crystallization behavior. GPC measurements were carried out on a Waters 150-C GPC equipped with TSK columns (Model GM-HXL-HT) at 135 °C with 1,2-dichlorobenzene as solvent. Monodisperse fractions of polystyrene were used as standards.

Solution ^{13}C NMR spectra were run at 75.4 MHz on a Varian UNITY-300 NMR spectrometer. Samples were run as 15% solutions in $C_2D_2Cl_4$ (TCE, Isotec) at 130 °C. Chemical shifts are referenced to TMS using as a secondary reference the methyl peak of polypropylene at 21.8 ppm. A total of 6000 transients were accumulated for each spectrum with a 12 s delay between pulses. Decoupling was always on during acquisition so the nuclear Overhauser enhancement was present.

Propene Concentration. The propene/toluene vapor–liquid equilibrium at 50 °C in the range 1–20.5 bar was estimated from the Redlich–Kwong–Soave equation. Propene concentration in the liquid phase has been calculated using the Rackett property. The agreement with the literature experimental data obtained at low pressure (1–5 atm)[38] is reasonably good (within ±3%). Propene concentrations in the range of interest are reported in the supporting information.

Method for the Evaluation of the Methyl Pentad Distribution from ^{13}C NMR Spectra in Which Overlapping with Peaks from End Groups and/or Regioirregular Units Occurs. The pentad distribution is calculated under the constraint that the polymerization statistic obeys pure enantiomorphic site control. As in the methyl pentad

region there are also peaks due to chain ends and isolated secondary units (2,1 and 1,3), the only peak areas which can be obtained with good precision are those of the four pentads mmmm, mmmr, mmrr, and mrrm. Furthermore, the mmmr pentad overlaps with the mmmm base; hence they can only be integrated together. The mmmm + mmmr areas have been corrected by subtracting the contribution from the vinylidene and *n*-propyl end groups.[39] The remaining pentads are of low intensity and overlapped to the above mentioned peaks.

On the other side, because of the relatively low catalyst isospecificity (especially at low monomer concentration), the contribution of the lesser pentads cannot be overlooked a priori when normalizing the experimental areas. To estimate this contribution, we proceed in the following way. The following expressions to calculate the pentad areas as a function of the *b* parameter have been employed (this parameter defines the probability of the "correct" insertion in the enantiomorphic site):[40]

$$\text{mmmm} + \text{mmmr} = (1-b)^5 + b^5 + 2(b(1-b)^4 + b^4(1-b)) \quad (10a)$$

$$\text{mmrr} = 2b^4(1-b) + 2b(1-b)^4 \quad (10b)$$

$$\text{mrrm} = b^4(1-b) + b(1-b)^4 \quad (10c)$$

The *b* value is searched with a least squares method, that is minimizing the square of the sum of the differences between the experimental areas and those calculated as a function of the *b* parameter.

Because these areas are not directly comparable, we can make them so by imposing that their sums are equal. To this purpose we utilize a proportionality constant *k*, calculated for each *b* value and defined as

$$k(b) = \frac{\sum \text{experimental areas}}{\sum \text{calculated areas}} \quad (11)$$

The function to be minimized is

$$f(b) = \sum_i (A_i^{\text{exp}} - kA_i^{\text{calc}})^2 \quad (12)$$

where A_i^{exp} are the experimental areas, A_i^{calc} are the calculated ones (through eqs 10a, 10b, and 10c) for each *b* value and the sum is extended over the three groups of pentads. The minimization process is carried out using the Microsoft Excel program.

Acknowledgment. We thank J. P. Faline and I. Camurati for the NMR spectra, D. Balboni for the catalyst synthesis, A. Celli and M. Cappati for thermal analysis, R. Agosti for GPC analysis, and A. Marzo for the viscosity measurements. We thank Professors U. Giannini, P. Corradini, and G. Guerra for stimulating discussions.

Supporting Information Available: GPC curve of sample 1, calculated curves of propylene concentration in toluene at 50 °C, flowchart for ^{13}C NMR data analysis and tables of experimental and calculated spectral areas, probability coefficients *b*, and least squares and calculated pentad distributions for samples **1**–**13** (6 pages). This material is contained in many libraries on microfiche, immediately follows this article in the microfilm version of the journal, and can be ordered from the American Chemical Society; see any current masthead page for ordering information.

Note Added in Proof. After this paper was submitted for publication, β-hydrogen transfer to the monomer after a secondary propene insertion was reported for a similar catalyst system.[41]

References and Notes

(1) Presented in part at the International Symposium on Synthetic, Structural, and Industrial Aspects of Stereospecific Polymerization (STEPOL '94), Milano, June 6–10, 1994; Book of Abstracts, p 205.

(2) (a) Ewen, J. *J. Am. Chem. Soc.* **1984**, *106*, 6355. (b) Ewen, J. U.S. Patent 4,522, 982 to Exxon, 1985. (c) Ewen, J. In *Catalytic Polymerization of Olefins, Studies in Surface Science and Catalysis*; Keii, T., Soga, K., Eds.; Elsevier: New York, 1986; Vol. 25, p 271. (d) Ewen, J.; Haspeslagh, L.; Atwood, J.; Zhang, H. *J. Am. Chem. Soc.* **1987**, *109*, 6544. (e) Ewen, J.; Haspeslagh, L.; Elder, M.; Atwood, J.; Zhang, H.; Cheng, H. In *Transition Metals and Organometallics as Catalysts for Olefin Polymerization*, Kaminsky, W., Sinn, H., Eds.; Springer-Verlag: Berlin, 1988; p 281.

(3) (a) Kaminsky, W.; Külper, K.; Brintzinger, H.; Wild, F. *Angew. Chem., Int. Ed. Engl.* **1985**, *24*, 507. (b) Kaminsky, W.; Külper, K.; Buschermöhle, M.; Lüker, H. U.S. Patent 4,-769,510 to Hoechst, 1988. (c) Kaminsky, W. *Angew. Makromol. Chem.* **1986**, *145/146*, 149. (d) Kaminsky, W. In *Catalytic Polymerization of Olefins*; Keii, T., Soga, K., Eds.; Elsevier: New York, 1986; p 293.

(4) (a) Schnutenhaus, H.; Brintzinger, H. H. *Angew. Chem., Int. Ed. Engl.* **1979**, *18*, 777. (b) Wild, F.; Zsolnai, L.; Huttner, G.; Brintzinger, H. H. *J. Organomet. Chem.* **1982**, *232*, 233. (c) Collins, S.; Kuntz, B.; Taylor, N.; Ward, D. *J. Organomet. Chem.* **1988**, *342*, 21. (d) Wild, F.; Wasiuchionek, M.; Huttner, G.; Brintzinger, H. H. *J. Organomet. Chem.* **1985**, *288*, 63. (e) Schäfer, A.; Karl, E.; Zsolnai, L.; Huttner, G.; Brintzinger, H. H. *J. Organomet. Chem.* **1987**, *328*, 87. (f) Wiesenfeldt, H.; Reinmuth, A.; Barsties, E.; Evertz, K.; Brintzinger, H. H. *J. Organomet. Chem.* **1989**, *369*, 359. (g) Burger, P.; Hortmann, K.; Diebold, J.; Brintzinger, H. H. *J. Organomet. Chem.* **1991**, *417*, 9. (h) Brintzinger, H. H. In *Transition Metals and Organometallics as Catalysts for Olefin Polymerization*; Kaminsky, W., Sinn, H., Eds.; Springer-Verlag: Berlin, 1988; p 249.

(5) (a) Corradini, P.; Guerra, G.; Vacatello, M.; Villani, V. *Gazz. Chim. Ital.* **1988**, *118*, 173. (b) Cavallo, L.; Guerra, G.; Oliva, L.; Vacatello, M.; Corradini, P. *Polym. Commun.* **1989**, *30*, 16. (c) Cavallo, L.; Corradini, P.; Guerra, G.; Vacatello, M. *Polymer* **1991**, *32*, 1329. (d) Cavallo, L.; Guerra, G.; Vacatello, M.; Corradini, P. *Chirality* **1991**, *3*, 299. (e) Guerra, G.; Cavallo, L.; Moscardi, G.; Vacatello, M.; Corradini, P. *J. Am. Chem. Soc.* **1994**, *116*, 2988.

(6) (a) Castonguay, L.; Rappé, A. *J. Am. Chem. Soc.* **1992**, *114*, 5832. (b) Hart, J.; Rappé, A. *J. Am. Chem. Soc.* **1993**, *115*, 6159. (c) Kawamura-Kuribayashi, H.; Koga, N.; Morokuma, K. *J. Am. Chem. Soc.* **1992**, *114*, 8687.

(7) A distinction must be made here between active *center* and reaction *site*: a metallocene-type active center (or active species) has a minimum of two sites (the two tetrahedral positions occupied by the two σ-ligands of the metallocene precatalyst) on which chain growth can take place. The nature of the reaction site is determined by the metal, the Cp ligand geometry, possible other ligands such as coordinated monomer or solvent, and the structure of the metal-bound chain end. As a result, the number of sites is increased by the different types of last inserted monomer unit (primary or secondary, *re* or *si* face).[5e] In the case of **1**, C_2 symmetry halves the number of different reaction sites. There are three different active sites which are present at different times during chain growth at each catalyst enantiomer: at the *R,R* enantiomer for example, a chain end can arise from primary *re* or *si* (P_{re}, P_{si} chain ends) or secondary *si* (S_{si} chain end) monomer insertions. At high monomer concentrations, these sites give rise to seven different propagation reactions, as 2,1 units are isolated (no S_{si} on S_{si}) and are only observed after P_{re} (no S_{si} on P_{si}). The different sites can be different in reactivity, regiospecificity, and enantioface selectivity, and as a result the active center itself changes during a single chain growth but *statistically* behaves in the same way from one polymer chain to the next. Thus such a species is a single-center catalyst. Hence, the denomination single-site catalysts used in connection with metallocene catalysts is incorrect and should be avoided.

(8) Eisch, J.; Piotrovsky, A.; Brownstein, S.; Gabe, E.; Lee, F. *J. Am. Chem. Soc.* **1985**, *107*, 7219.

(9) (a) Jordan, R.; Bajgur, C.; Willet, R.; Scott, B. *J. Am. Chem. Soc.* **1986**, *108*, 7410. (b) Jordan, R.; LaPointe, R.; Bajgur,

C.; Echols, S.; Willet, R. *J. Am. Chem. Soc.* **1987**, *109*, 4111. (c) Jordan, R. *J. Chem. Educ.* **1988**, *65*, 285.

(10) See for example: (a) Pino, P.; Cioni, P.; Wey, J. *J. Am. Chem. Soc.* **1987**, *109*, 6189. (b) Pino, P.; Cioni, P.; Galimberti, M.; Wei, J.; Piccolrovazzi, N. In *Transition Metals and Organometallics as Catalysts for Olefin Polymerization*; Kaminsky, W., Sinn, H., Eds.; Springer-Verlag: Berlin, 1988; p 269. (c) Pino, P.; Galimberti, M. *J. Organomet. Chem.* **1989**, *370*, 1. (d) Ewen, J.; Elder, M.; Jones, R.; Haspeslagh, L.; Atwood, J.; Bott, S.; Robinson, K. *Makromol. Chem., Macromol. Symp.* **1991**, *48/49*, 253. (e) Horton, A.; Frijns, J. *Angew. Chem., Int. Ed. Engl.* **1991**, *30*, 1152. (f) Chien, J.; Tsai, W.; Rausch, M. *J. Am. Chem. Soc.* **1991**, *113*, 8570. (g) Bochmann, M.; Lancaster, S. *Organometallics* **1993**, *12*, 633.

(11) These are found to produce iPP which is not suitable for current commercial applications: at practical polymerization temperatures, in fact, molecular weight, isotacticity, and regioregularity are relatively low, and these molecular properties are reflected in very high solvent solubilities, low melting temperatures, and poor mechanical properties.[12] For comparison with commercial grade iPP, see, for example: (a) Martuscelli, E.; Pracella, M.; Zambelli, A. *J. Polym. Sci., Polym. Phys.* **1980**, *18*, 619. (b) Martuscelli, E.; Avella, M.; Segre, A. L.; Rossi, E.; Di Drusco, G.; Galli, P.; Simonazzi, T. *Polymer* **1985**, *26*, 259. (c) Barbé, P. C.; Cecchin, G.; Noristi, L. *Adv. Polym. Sci.* **1987**, *81*, 1. (d) van der Ven, Ser. *Polypropylene and other polyolefins, Studies in Polymer Science*; Elsevier: New York, 1990; Vol. 7, pp 1–212. (e) Cheng, S.; Janimak, J.; Zhang, A.; Hsieh, E. *Polymer* **1991**, *32*, 648. (f) Sacchi, M. C.; Forlini, F.; Tritto, I.; Mendichi, R.; Zannoni, G.; Noristi, L. *Macromolecules* **1992**, *25*, 5914.

(12) (a) Soga, K.; Shiono, T.; Takemura, S.; Kaminsky, W. *Makromol. Chem., Rapid Commun.* **1987**, *8*, 305. (b) Grassi, A.; Zambelli, A.; Resconi, L.; Albizzati, E.; Mazzocchi, R. *Macromolecules* **1988**, *21*, 617. (c) Cheng, H.; Ewen, J. *Makromol. Chem.* **1989**, *190*, 1931. (d) Tsutsui, T.; Ishimaru, N.; Mizuno, A.; Toyota, A.; Kashiwa, N. *Polymer* **1989**, *30*, 1350. (e) Tsutsui, T.; Mizuno, A.; Kashiwa, N. *Makromol. Chem.* **1989**, *190*, 1177. (f) Tsutsui, T.; Kioka, M.; Toyota, A.; Kashiwa, N. In *Catalytic Olefin Polymerization, Studies in Surface Science and Catalysis*; Keii, T., Soga, K., Eds.; Elsevier: New York, 1990; Vol. 56, p 493. (g) Rieger, B.; Chien, J. *Polym. Bull.* **1989**, *21*, 159. (h) Rieger, B.; Mu, X.; Mallin, D.; Rausch, M.; Chien, J. *Macromolecules* **1990**, *23*, 3559. (i) Chien, J.; Sugimoto, R. *J. Polym. Sci., Part A: Polym. Chem.* **1991**, *29*, 459.

(13) (a) Mise, T.; Miya, S.; Yamazaki, H. *Chem. Lett.* **1989**, 1853. (b) Röll, W.; Brintzinger, H.; Rieger, B.; Zolk, R. *Angew. Chem., Int. Ed. Engl.* **1990**, *29*, 279. (c) Collins, S.; Gauthier, W.; Holden, D.; Kuntz, B.; Taylor, N.; Ward, D. *Organometallics* **1991**, *10*, 2061. (d) Rieger, B. *J. Organomet. Chem.* **1992**, *428*, C33. (e) Kaminsky, W.; Engehausen, R.; Zoumis, K.; Spaleck, W.; Rohrmann, J. *Makromol. Chem.* **1992**, *193*, 1643. (f) Spaleck, W.; Küber, F.; Winter, A.; Rohrmann, J.; Bachmann, B.; Antberg, M.; Dolle, V.; Paulus, E. *Organometallics* **1994**, *13*, 954.

(14) (a) Drögemüller, H.; Niedoba, S.; Kaminsky, W. *Polym. React. Eng.* **1986**, 299. (b) Tsutsui, T.; Kashiwa, N.; Mizuno, A. *Makromol. Chem., Rapid Commun.* **1990**, *11*, 565. (c) Huang, J.; Rempel, G. *Stud. Surf. Sci. Catal.* **1992**, *73*, 169. (d) Busico, V.; Cipullo, R.; Corradini, P. *Makromol. Chem., Rapid Commun.* **1993**, *14*, 97. (e) Fisher, D.; Jüngling, S.; Mülhaupt, R. *Makromol. Chem., Macromol. Symp.* **1993**, *66*, 191.

(15) Rieger, B.; Jany, G.; Fawzi, R.; Steimann, M. *Organometallics* **1994**, *13*, 647.

(16) Stehling, U.; Diebold, J.; Kirsten, R.; Röll, W.; Brintzinger, H. H.; Jüngling, S.; Mülhaupt, R.; Langhauser, F. *Organometallics* **1994**, *13*, 964.

(17) A similar effect on isotacticity has also been observed with other zirconocene catalysts. (a) Busico, V. Oral presentation at the International Symposium on Synthetic, Structural, and Industrial Aspects of Stereospecific Polymerization (STEPOL '94), Milano, June 6–10, 1994. (b) Busico, V.; Cipullo, R. *J. Am. Chem. Soc.* **1994**, *116*, 9329. (c) Busico, V.; Cipullo, R.; Chadwick, J. C.; Modder, J. F.; Sudmeijer, O. *Macromolecules* **1994**, *27*, 7538.

(18) Kaminsky, W.; Ahlers, A.; Möller-Lindenhof, N. *Angew. Chem., Int. Ed. Engl.* **1989**, *28*, 1216.

(19) Ewen, J. A.; Elder, M. J.; Jones, R. L.; Curtis, S.; Cheng, H. N. In *Catalytic Olefin Polymerization, Studies in Surface Science and Catalysis*; Keii, T., Soga, K., Eds.; Elsevier: New York, 1990; Vol. 56, p 439.

(20) Herfert, N.; Fink, G. *Makromol. Chem.* **1992**, *193*, 773.

(21) Leclerc, M. K.; Brintzinger, H. H. *J. Am. Chem. Soc.* **1995**, *117*, 1651.

(22) Suter, U. W.; Neuenschwander, P. *Macromolecules* **1981**, *14*, 528.

(23) The correct nomenclature for these structures should be secondary meso and secondary racemic. We use here Zambelli's nomenclature,[12b] erythro (E) and threo (T), respectively, to avoid confusion with m, r dyad definition.

(24) Mizuno, A.; Tsutsui, T.; Kashiwa, N. *Polymer* **1992**, *33*, 254.

(25) Grassi, A.; Ammendola, P.; Longo, P.; Albizzati, E.; Resconi, L.; Mazzocchi, R. *Gazz. Chim. Ital.* **1988**, *118*, 539.

(26) Tsutsui, T.; Kashiwa, N.; Mizuno, A. *Makromol. Chem., Rapid Commun.* **1990**, *11*, 565. Busico, V.; Cipullo, R.; Corradini, P. *Makromol. Chem., Rapid Commun.* **1993**, *14*, 97.

(27) Herfert, N.; Fink, G. *Makromol. Chem., Macromol. Symp.* **1993**, *66*, 157. Fink, G.; Herfert, N.; Montag, P. In *Ziegler Catalysts*; Fink, G., Mülhaupt, R., Brintzinger, H. H., Eds.; Springer-Verlag: Berlin, 1995; p 159.

(28) Fisher, D.; Mülhaupt, R. *J. Organomet. Chem.* **1991**, *417*, C7.

(29) Resconi, L.; Piemontesi, F.; Franciscono, G.; Abis, L.; Fiorani, T. *J. Am. Chem. Soc.* **1992**, *114*, 1025.

(30) (a) Chien, J. C. W.; Wang, B. P. *J. Polym. Sci., Part A: Polym. Chem.* **1988**, *26*, 3089. (b) Chien, J. C. W.; Razavi, A. *J. Polym. Sci., Part A: Polym. Chem.* **1988**, *26*, 2369. (c) Chien, J. C. W.; Wang, B. P. *J. Polym. Sci., Part A: Polym. Chem.* **1990**, *28*, 15. (d) Resconi, L.; Bossi, S.; Abis, L. *Macromolecules* **1990**, *23*, 4489.

(31) (a) Tsutsui, T.; Mizuno, A.; Kashiwa, N. *Polymer* **1989**, *30*, 428. (b) Randall, J.; Rucker, S. *Macromolecules* **1994**, *27*, 2120.

(32) Shiono, T.; Soga, K. *Macromolecules* **1992**, *25*, 3356.

(33) Zambelli, A.; Locatelli, P.; Zannoni, G.; Bovey, F. A. *Macromolecules* **1978**, *11*, 923.

(34) Resconi, L.; Abis, L.; Franciscono, G. *Macromolecules* **1992**, *25*, 6814.

(35) Lee, J.; Gauthier, W.; Ball, J.; Iyengar, B.; Collins, S. *Organometallics* **1992**, *11*, 2115.

(36) Piemontesi, F.; Camurati, I.; Resconi, L.; Balboni, D.; Sironi, A.; Moret, M.; Zeigler, R.; Piccolrovazzi, N. *Organometallics* **1995**, *14*, 1256.

(37) Moraglio, G.; Gianotti, G.; Bonicelli, U. *Eur. Polym. J.* **1973**, *9*, 693.

(38) von Frank, H. P. *Öst. Chem. Z.* **1967**, *68*, 360. Hannaert, H.; Haccuria, M.; Mathieu, M. P. *Ind. Chim. Belg.* **1967**, *2*, 156.

(39) Rieger, B.; Reinmuth, A.; Röll, W.; Brintzinger, H. H. *J. Mol. Catal.* **1993**, *82*, 67.

(40) v.d. Burg, M.; Chadwick, J.; Sudmeijer, O.; Tulleken, H. *Makromol. Chem., Theory Simul.* **1993**, *2*, 399 and references therein.

(41) Jüngling, S.; Mülhaupt, R.; Stehling, U.; Brintzinger, H. H.; Fisher, D.; Langhauser, F. *J. Polym. Sci., Part A: Polym. Chem.* **1995**, *33*, 1305.

MA950766X